Schwann cells expressing dismutase active mutant SOD1 unexpectedly slow disease progression in ALS mice

Christian S. Lobsiger[a,b,c,d], Severine Boillee[a,b,c,d], Melissa McAlonis-Downes[a], Amir M. Khan[a], M. Laura Feltri[e], Koji Yamanaka[a,f,1], and Don W. Cleveland[a,2]

[a]Department of Medicine and Neuroscience, Ludwig Institute for Cancer Research, University of California at San Diego, La Jolla, CA 92093; [b]Institut National de la Santé et de la Recherche Médicale, Unité Mixte de Recherche S975, Centre de Recherche de l'Institut du Cerveau et de la Moelle Épinière, Hôpital de la Salpêtrière, 75013 Paris, France; [c]Université Pierre et Marie Curie Paris 6, 75013 Paris, France; [d]Centre National de la Recherche Scientifique, Unité Mixte de Recherche 7225, 75013 Paris, France; [e]Department of Cell Biology and Genetics, San Raffaele Scientific Research Institute, 20132 Milan, Italy; and [f]Yamanaka Research Unit, RIKEN Brain Science Institute, Saitama 351-0198, Japan

Contributed by Don W. Cleveland, December 30, 2008 (sent for review December 15, 2008)

Neurodegeneration in an inherited form of ALS is non-cell-autonomous, with ALS-causing mutant SOD1 damage developed within multiple cell types. Selective inactivation within motor neurons of an ubiquitously expressed mutant *SOD1* gene has demonstrated that mutant damage within motor neurons is a determinant of disease initiation, whereas mutant synthesis within neighboring astrocytes or microglia accelerates disease progression. We now report the surprising finding that diminished synthesis (by 70%) within Schwann cells of a fully dismutase active ALS-linked mutant ($SOD1^{G37R}$) significantly accelerates disease progression, accompanied by reduction of insulin-like growth factor 1 (IGF-1) in nerves. Coupled with shorter disease duration in mouse models caused by dismutase inactive versus dismutase active SOD1 mutants, our findings implicate an oxidative cascade during disease progression that is triggered within axon ensheathing Schwann cells and that can be ameliorated by elevated dismutase activity. Thus, therapeutic down-regulation of dismutase active mutant SOD1 in familial forms of ALS should be targeted away from Schwann cells.

neurodegeneration | non-cell-autonomous | superoxide dismutase | amyotrophic lateral sclerosis | motor neurons

Amyotrophic lateral sclerosis (ALS) is a fatal, adult-onset neurodegenerative disease that causes premature death of brain and spinal cord motor neurons (1). Most cases of ALS are of unknown etiology, but some familial forms are linked to dominant missense mutations in the ubiquitously expressed *SOD1* (superoxide dismutase 1) gene (1). SOD1 is an abundant intracellular anti-oxidant, which converts superoxide radicals in the cytoplasm to hydrogen peroxide (which is then further converted by peroxidases to water). Its known activity initially lead to the hypothesis that reduced SOD1 activity could drive motor neuron degeneration in ALS via increased oxidative stress (2). However, transgenic mice develop ALS-like motor neuron degeneration through ubiquitous expression of either dismutase *active* or *inactive* mutant SOD1 forms. Although neither increased expression of wild-type SOD1 nor deletion of endogenous SOD1 cause motor neuron disease (1), evidence has lead to the conclusion that disease is caused by a novel acquired toxicity of mutant SOD1 independent of its dismutase activity (1).

Prominent models proposed for the nature of SOD1-linked ALS toxicity, include intraastrocytic damage from it leading to loss of the EAAT2 glutamate transporter (3), aberrant association with mitochondria (4), aberrant cosecretion with chromogranin (5), sustained activation of NADPH oxidase (6, 7), and inhibition of the ERAD pathway for removal of misfolded proteins (8). Whichever of these are correct, evidence from many directions has demonstrated that toxicity is non-cell-autonomous, with mutant-mediated damage generated within multiple cell types, including the affected motor neurons but also by their neighboring astrocytes and microglia. Initial evidence for non-cell autonomy came from analysis of chimeric mice, which demonstrated a protective effect of wild-type cells surrounding mutant SOD1 expressing motor neurons (9). By using cell type specific Cre-mediated gene excision, it was then shown that reducing mutant SOD1 expression in motor neurons delayed disease initiation (10), although similar mutant reduction in either microglia (10) or astrocytes (11) slowed disease progression. A contribution of mutant expressing astrocytes to driving death of human (7, 12) or mouse (13, 14) motor neurons has also been seen in vitro.

Because in the spinal cord, microglia and astrocytes represent the major nonneuronal cell types associated with motor neurons, a contribution from them in driving disease mechanism may not, in retrospect, be surprising. In the periphery, however, although mutant synthesis solely in muscle, the motor neuron targets, can provoke damage to those muscles (15), this apparently plays little role in disease mechanism. Reduction of mutant SOD1 synthesis in the skeletal muscle of ALS mice does not affect disease onset or progression (16).

Possible damage within or to the Schwann cells, the myelinating glia of the peripheral nervous system, has not been examined so far, despite the fact that they are associated with the full length of peripheral axons (which represent 90% of the volume of motor neurons). Highlighting the potential for a contribution from them in ALS is the fact that in contrast to a 15:1–20:1 ratio of central nervous system glia surrounding the motor neuron perikaryon, the ratio of Schwann cells to a single motor axon is 1,000:1 (17). Schwann cells form an intimate bidirectional relationship with their neuronal partners: during development Schwann cells are essential for the survival of motor neurons, whereas neuron-derived factors guide survival and differentiation of Schwann cells along axons (18). These interactions become again important during neuronal regeneration (19, 20). Schwann cells distal to the injury do not die, rather they shed off and phagocytose (together with macrophages) their myelin sheets and then enter a dedifferentiation/redifferentiation program to guide and support the regrowing axon followed ultimately by remyelination of it. Further, in

Author contributions: C.S.L. and D.W.C. designed research; C.S.L., S.B., M.M.-D., A.M.K., and K.Y. performed research; M.L.F. and K.Y. contributed new reagents/analytic tools; C.S.L. and D.W.C. analyzed data; and C.S.L. and D.W.C. wrote the paper.

The authors declare no conflict of interest.

[1]Present address: Core Research for Evolutional Science and Technology, Japan Science and Technology Corporation, Bunkyo, Tokyo 113-0033, Japan.

[2]To whom correspondence should be addressed. E-mail: dcleveland@ucsd.edu.

This article contains supporting information online at www.pnas.org/cgi/content/full/0813339106/DCSupplemental.

certain forms of Charcot-Marie-Tooth peripheral neuropathies, disease toxicity is directly linked to mutations in genes encoding Schwann cell myelin components (21), resulting in demyelination and even secondary axonal degeneration.

However, surprisingly little is known about a contribution, if any, of Schwann cells in ALS. Studies from human ALS have described myelin alterations along the peripheral nerves (22), most likely secondary due to massive axonal degeneration. At neuromuscular junctions in ALS mice, a recent study reported induction of the axon repellent semaphorin 3A in terminal Schwann cells (23) (a subpopulation of Schwann cells important for synaptic support and regeneration), suggesting either a detrimental or physiologic response to ongoing denervation (24). All of this raises the question of whether Schwann cells in ALS actively contribute to motor neuron degeneration or whether they are merely bystanders to the ongoing neurodegenerative process.

To assess the role of Schwann cells in ALS in a first global approach, we focus here on their contribution to non-cell-autonomous mutant SOD1-linked ALS toxicity. With the known capacity of Schwann cells to respond to axonal damage and produce various neurotrophic factors (19), we hypothesized that mutant SOD1 expression disturbs normal Schwann cell functions, especially during disease progression, which is defined by axonal degeneration and regenerative and/or compensatory attempts of surviving motor neurons (24, 25). Therefore, we have used Cre-mediated gene excision in ALS mice (10) to remove mutant SOD1 specifically from Schwann cells.

Results

Efficient Cre-Mediated Mutant *SOD1* Gene Excision in Schwann Cells of ALS Mice. To assess the contribution of Schwann cell-expressed mutant SOD1 to non-cell-autonomous ALS toxicity, we mated mice heterozygous for a mutant human $SOD1^{G37R}$ transgene flanked by loxP sites (LoxSOD1^{G37R} mice) that develop progressive and fatal ALS-like motor neuron degeneration (10) with mice expressing the Cre recombinase under the control of mouse myelin-protein-zero (P_0) regulatory sequences (26). P_0-cre mice are well-established to excise floxed genes almost exclusively from peripheral myelinating or nonmyelinating Schwann cells without targeting central nervous system myelinating glia (oligodendrocytes) or other central or peripheral neurons or glia (26, 27). By mating P_0-cre mice with Cre-inducible ROSA26-β-galactosidase (β-Gal) reporter mice (10, 11), we confirmed this selectivity, demonstrating β-Gal activity in most sciatic nerve Schwann cells (Fig. 1*A* and *B*) but none in spinal cord cells (Fig. 1*D*). Because one report suggested the potential involvement of terminal Schwann cells in ALS (23), we also confirmed P_0-cre activity in many of these specialized, S100-positive, unmyelinating Schwann cells, which are closely apposed to nerve terminal branches at neuromuscular junctions (Fig. 1*C*) (30–50% were β-Gal positive; D. Hess, R. Balice-Gordon, M.L. Feltri, and L. Wrabetz, personal communication).

P_0-cre-mediated $SOD1^{G37R}$ transgene excision in Schwann cells was highly efficient. By using real-time PCR (qPCR) on sciatic nerve tissue extracts (containing genomic DNA derived almost exclusively from Schwann cells), a 70% reduction of $SOD1^{G37R}$ transgene levels in LoxSOD1^{G37R}/P_0-cre mice was identified, with no significant reduction in spinal cord tissue (Fig. 1*E*). Mutant $SOD1^{G37R}$ mRNA levels were also reduced by a comparable 70% (Fig. 1*F*). Considering that the nerve also contains some (P_0-cre negative) perineurial and endothelial cells (18), the actual excision rate in Schwann cells is probably nearly complete.

Schwann Cell-Expressed Dismutase Active Mutant SOD1 Is Neuroprotective as Its Removal Reduces Survival. To assess the effect of Schwann cell-specific removal of mutant SOD1 in ALS mice, we compared disease courses between LoxSOD1^{G37R}/P_0-cre mice and LoxSOD1^{G37R} littermates. Both LoxSOD1^{G37R} and P_0-cre lines were in congenic C57BL/6 grounds. A presymptomatic phase was defined by the period of weight gain typical for young adult mice. Earliest disease onset was defined by the age at the inflection point in the weight curve. An early symptomatic phase was characterized by gait alterations, reduced grip strength, and denervation-induced muscle atrophy (10, 11, 28), that last of which was responsible for weight loss. A simple, objective early disease point was defined by the time at which weight loss reached 10% of peak weight, a measure repeatedly used previously in ALS mice (10, 11, 28, 29). Further symptomatic progression resulted in paralysis at end stage disease (29).

Despite efficient removal of mutant SOD1 from Schwann cells, disease onset was not significantly different between LoxSOD1^{G37R}/P_0-cre (8.2 months; 249 ± 11.2 days (d); n = 20) and LoxSOD1^{G37R} (8.5 months; 259 ± 9.9 d; n = 19) mice (Fig.

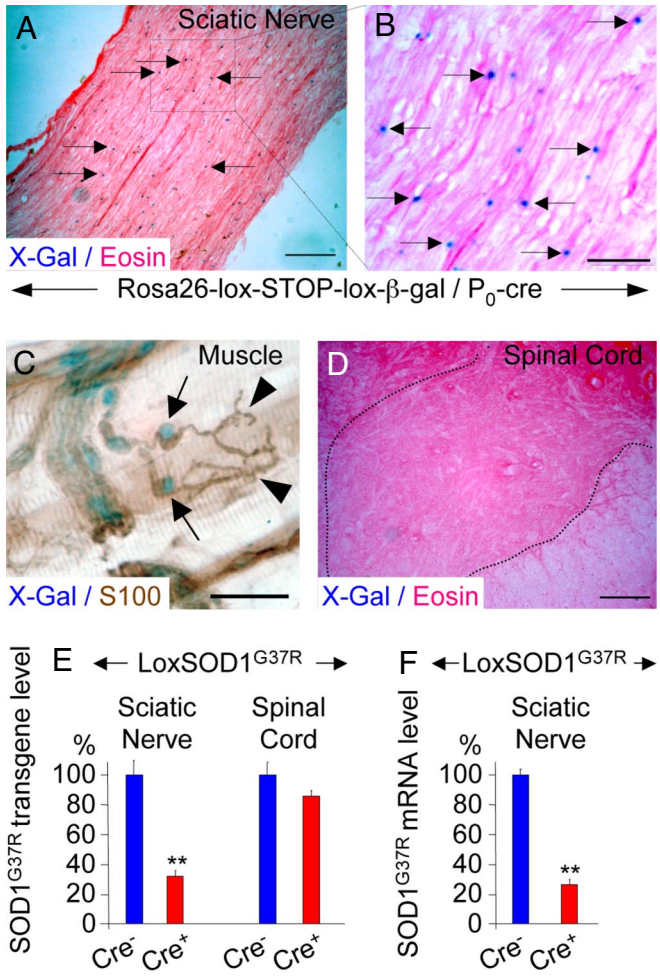

Fig. 1. Targeted P_0-cre-mediated gene excision in LoxSOD1^{G37R} ALS mice was used to specifically reduce Schwann cell-expressed mutant SOD1. (*A–D*) β-galactosidase (β-Gal) activity in Schwann cells (*A* and *B*, arrows) of longitudinal sciatic nerve sections, as well as in terminal Schwann cells (*C*, arrows; visualized with S100 immunostaining) at the neuromuscular junction (arrowheads) of gastrocnemius muscles but not in (*D*) spinal cord glia or neurons of (*A–D*) adult ROSA26/P_0-Cre reporter mice, visualized with X-Gal (*A–D*) and counterstained with eosin (*A*, *B*, and *D*). [Scale bars: 100 μm (*A* and *D*); 30 μm (*B* and *C*).] (*E* and *F*) qPCR showing a 70% reduction of human $SOD1^{G37R}$ transgene (*E*) and mRNA (*F*) levels ($P < 0.01$; Student's t test) in sciatic nerves of LoxSOD1^{G37R}/P_0-cre (Cre$^+$) mice relative to LoxSOD1^{G37R} (Cre$^-$) littermates, without significant spinal cord $SOD1^{G37R}$ transgene reduction (*E*) (n = 3 mice per group; presymptomatic, 4 months old; error bars, SEM).

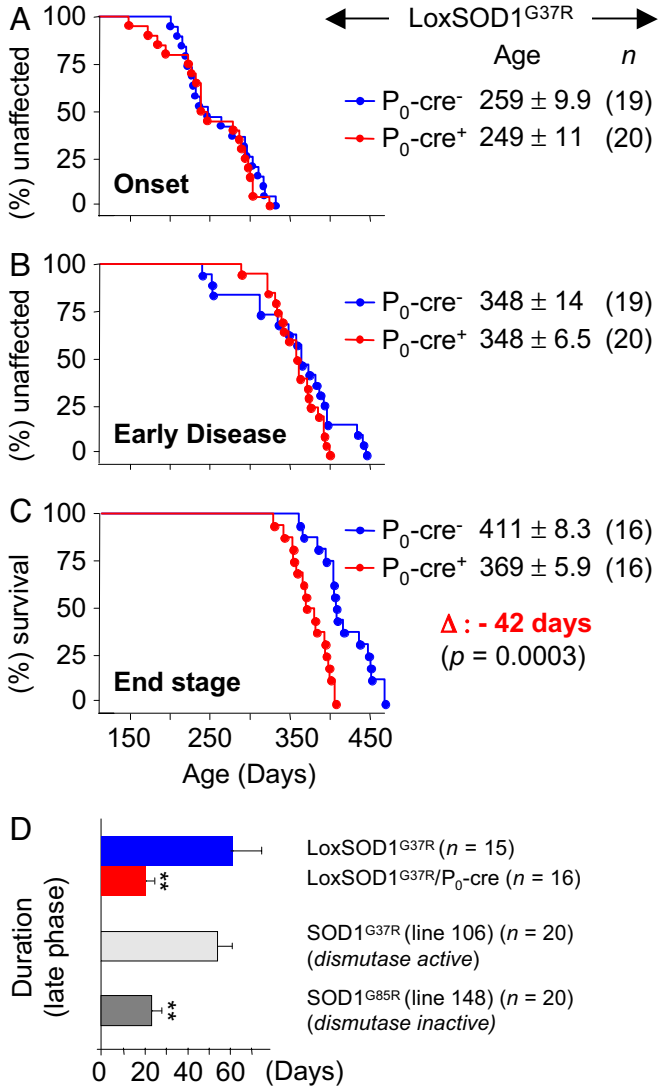

Fig. 2. Selective mutant *SOD1* gene excision from Schwann cells accelerates disease progression in ALS mice. (*A–C*) Plots of ages (in days) at which disease onset (*A*), early disease (*B*), and end stage (*C*) are reached in LoxSOD1^{G37R} ALS mice with (blue) and without (red) mutant SOD1 in Schwann cells. (*D*) Correlation between dismutase activity of Schwann cell-localized SOD1 mutants with slow disease progression in ALS mice: removal of dismutase *active* mutant SOD1^{G37R} from Schwann cells leads to a 3-fold faster late phase (from early disease to end stage) in LoxSOD1^{G37R}/P$_0$-cre mice than in LoxSOD1^{G37R} mice ($P < 0.01$; Student's *t* test). This difference correlates well with a faster late phase in dismutase inactive mutant SOD1^{G85R} mice (line 148; end stage at 12.5 months) as compared to a slow late phase in dismutase active mutant SOD1^{G37R} mice (line 106; end stage at 13.5 months) ($P < 0.001$; Student's *t* test) (see *Discussion*).

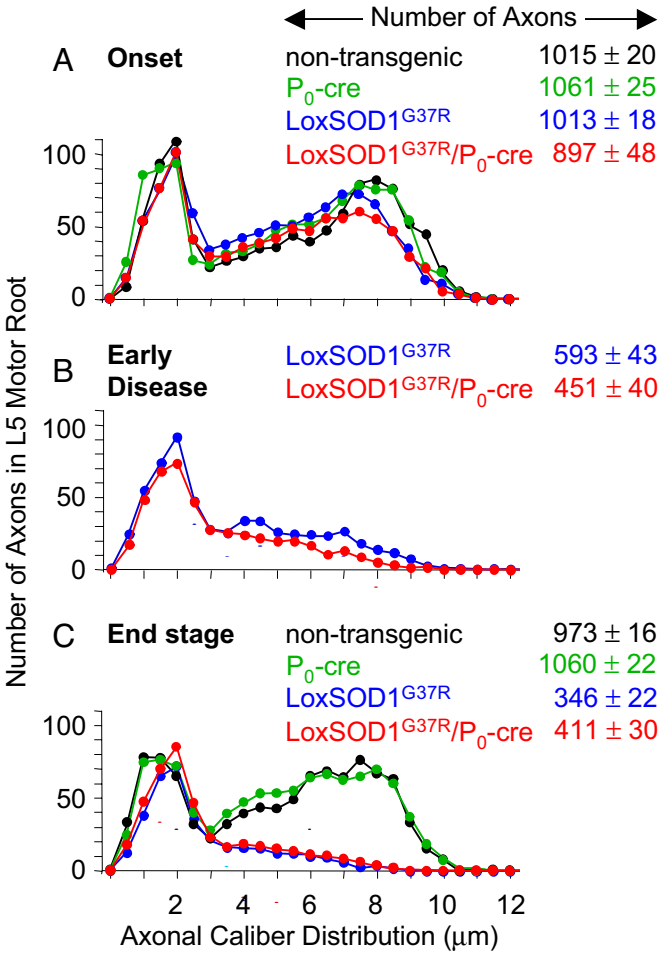

Fig. 3. Assessment of axonal degeneration in lumbar motor roots of ALS mice with or without Cre-mediated mutant *SOD1* excision in Schwann cells. Numbers and distributions of axonal diameters in L5 motor roots of LoxSOD1^{G37R} and LoxSOD1^{G37R}/P$_0$-cre mice at onset (8.5 months) (*A*), early disease (*B*), and end stage (*C*). No axonal degeneration was seen in nontransgenic or single transgenic P$_0$-cre control mice at ages matched to onset (8.5 months) or end stage (13.5 months) (*A* and *C*) ($n = 4$ mice per group; error, SEM).

2*A*). Likewise, the age at which disease progressed to early phenotypic disease was similar in LoxSOD1^{G37R}/P$_0$-cre (11.5 months; 348 ± 6.5 d; $n = 20$) and LoxSOD1^{G37R} (11.5 months; 348 ± 14.0 d; $n = 19$) mice (Fig. 2*B*). Very surprisingly, however, removal of mutant SOD1^{G37R} from Schwann cells significantly reduced survival by accelerating disease progression after this early disease stage. End stage for LoxSOD1^{G37R}/P$_0$-cre mice was reached 42 days (1.4 months) earlier than for LoxSOD1^{G37R} mice (12.1 months; 369 ± 5.9 d; $n = 16$ versus 13.5 months; 411 ± 8.3 d; $n = 16$; $P = 0.0003$; Student's *t* test) (Fig. 2*C*). An "early phase" of disease progression (from onset through early phenotypic disease) was unchanged between LoxSOD1^{G37R}/P$_0$-cre (99 ± 9.8 d; $n = 20$) and LoxSOD1^{G37R} mice (89 ± 13.8 d; $n = 19$) (Fig. 2 *A* and *B*). However, progression through the "late phase" of disease was significantly accelerated (by almost 3 fold; Fig. 2 *C* and *D*) in LoxSOD1^{G37R}/P$_0$-cre mice (20.9 ± 3.6 d, $n = 16$) as compared with LoxSOD1^{G37R} mice (61.7 ± 12.9 d, $n = 15$; $P < 0.01$; Student's *t* test) (Fig. 2*D*), suggesting a link between slow disease progression in ALS mice and a protective effect of dismutase active mutant SOD1 in Schwann cells (Fig. 2*D*).

To determine how removal of mutant SOD1^{G37R} from Schwann cells influenced degenerative processes in ALS mice, we first confirmed motor axon integrity (Fig. 3 *A* and *C* and supporting information (SI) Fig. S1) and observed normal axon calibers and myelin thickness (Fig. S2) in young and aged P$_0$-cre control mice. We then compared the extent of motor axonal degeneration at similar disease-stages in mutant SOD1 mice. We found that in LoxSOD1^{G37R} mice (with or without P$_0$-cre), major axonal degeneration started after onset (Fig. 3 and Fig. S1) and was accompanied by secondary myelin alterations (Fig. S2 and Fig. S3). At all 3 disease stages analyzed (onset, early disease, and end stage) there were no significant differences between LoxSOD1^{G37R}/P$_0$-cre and LoxSOD1^{G37R} mice, either with respect to axonal loss or caliber reduction (Fig. 3 and Fig. S1) or for overall axonal or myelin pathology (Fig. S2 and Fig. S3). This

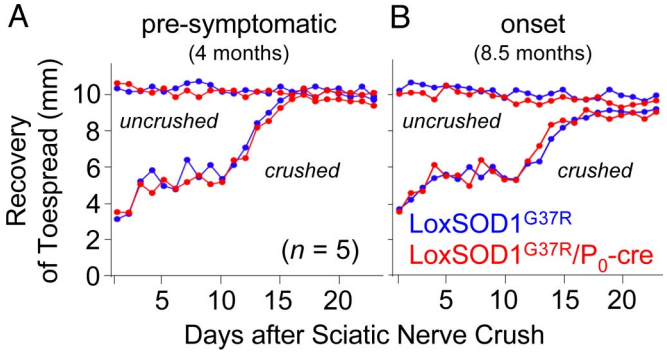

Fig. 4. The inherent regenerative capacity of motor neurons after crush injury is not influenced by Schwann cell-expressed mutant SOD1. The speed of nerve regeneration (measured by the toe spread) after unilateral crush injury was assessed at 2 time points [at 4 months (*A*), presymptomatic, and at 8.5 months (*B*), onset] before the appearance of overall symptoms (at 11.5 months). No significant differences were detected between LoxSOD1^{G37R}/P_0-cre and LoxSOD1^{G37R} ALS mice (n = 5 mice per group; only males used), indicating that removal of mutant SOD1^{G37R} from Schwann cells did not influence the sciatic nerve's inherent regenerative capacity (similar results were obtained with females; Fig. S4*A*).

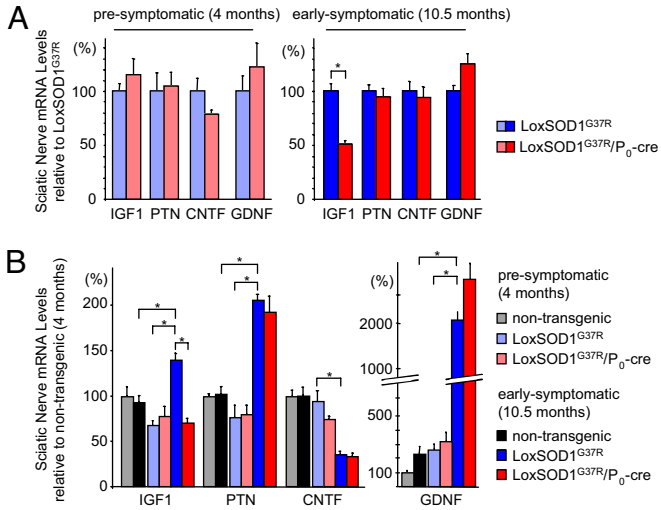

Fig. 5. More aggressive disease progression in ALS mice with reduced Schwann cell-expressed mutant SOD1 is accompanied by reduced IGF-1. (*A*) By using RT-qPCR analysis, whole sciatic nerve mRNA expression levels of IGF-1, PTN, CNTF, and GDNF are compared between LoxSOD1^{G37R}/P_0-cre and LoxSOD1^{G37R} ALS mice at presymptomatic and early symptomatic disease stages. At an early symptomatic time point (10.5 months), removal of dismutase active mutant SOD1^{G37R} from Schwann cells leads to a 50% reduction ($P < 0.05$; Student's t test) selectively of IGF-1 in LoxSOD1^{G37R}/P_0-cre ALS-mice. (*B*) Comparison of mRNA levels from presymptomatic and early symptomatic ages in LoxSOD1^{G37R} ALS mice: disease-associated inductions are found for IGF-1 (2.0-fold), PTN (2.7-fold), and GDNF (8.6-fold), whereas CNTF is reduced (2.3-fold) ($P < 0.05$; Student's t test). There is no disease-associated IGF-1 induction after removal of mutant SOD1 from Schwann cells. Absolute inductions of IGF-1 and PTN in early symptomatic LoxSOD1^{G37R} ALS mice as compared with age-matched (nontransgenic) control mice are 1.5-fold and 2.0-fold, respectively ($P < 0.05$; Student's t test) (n = 3 mice per group; error bars, SEM).

is consistent with a true faster axonal degeneration in the late phase of disease progression in LoxSOD1^{G37R}/P_0-cre mice, as they reached end stage (after early disease) 3 times more quickly than LoxSOD1^{G37R} mice but showed a similar high degree of axonal degeneration at each stage. There was even a trend of increased axonal loss already at early disease in LoxSOD1^{G37R}/P_0-cre mice (Fig. S1), suggesting that acceleration of progression starts at or just before our definition of early disease.

The Inherent Regenerative Capacity of Motor Neurons After Crush Injury Is Not Influenced by Schwann Cell-Expressed Mutant SOD1. Schwann cells are involved in successful axonal regeneration (19) and during disease progression in ALS mice, there are active attempts at neuronal regeneration and/or compensation (24, 25). As wild-type SOD1 has been shown to be neuroprotective in neural injury paradigms (30, 31), we hypothesized that the decrease in overall dismutase activity from removal of dismutase active mutant SOD1^{G37R} from Schwann cells could thereby decrease the nerve's inherent capacity for regeneration. Therefore, we crushed sciatic nerves at 2 time points (4 and 8.5 months of age), before appearance of overall symptoms (at ≈11.5 months), and compared functional regeneration between LoxSOD1^{G37R}/P_0-cre and LoxSOD1^{G37R} mice. To avoid bias due to known neuroprotective effects of estrogen (32), genders were analyzed separately. No significant differences were found in regeneration when comparing LoxSOD1^{G37R}/P_0-cre and LoxSOD1^{G37R} mice (Fig. 4 and Fig. S4 *A* and *B*). In both, however, there was a trend to slower regeneration when comparing the 8.5- to the 4-month-old ALS mice (Fig. 4 *A* and *B*; Fig. S4*C*), consistent with recent data showing a disease-linked slowing of nerve regeneration in a different line of SOD1 mutant mice (24).

More Aggressive Disease Progression in ALS Mice with Reduced Schwann Cell-Expressed Mutant SOD1 is Accompanied by Reduced IGF-1. To test if the presence or absence of dismutase active mutant SOD1 within Schwann cells affected the known regeneration-associated capacity of Schwann cells to induce diverse neurotrophic factors (19), we assessed the expression of 4 potent motor neurotrophic factors: insulin-like growth factor 1 (IGF-1), pleiotrophin (PTN), ciliary neurotrophic factor (CNTF), and glial-derived neurotrophic factor (GDNF). Analysis of sciatic nerve mRNAs by RT-qPCR (normalized to LoxSOD1^{G37R} mice) revealed that removal of mutant SOD1^{G37R} from Schwann cells did not lead to changes in inherent IGF-1, PTN, CNTF, or GDNF expression levels presymptomatically (at 4 months) (Fig. 5*A*), consistent with similar regenerative capacities after crush injury (Fig. 4*A*). However, at an early symptomatic age (10.5 months) and shortly before reaching our early phenotypic disease mark (10% weight loss at ≈11.5 months), sciatic nerve Schwann cell-derived IGF-1 levels were reduced almost 50% ($P < 0.05$; Student's t test) in LoxSOD1^{G37R}/P_0-cre mice as compared with age-matched LoxSOD1^{G37R} mice (Fig. 5*A*). This loss was selective for IGF-1, as no differences were detected for PTN, CNTF, or GDNF (Fig. 5*A*).

Relative to the levels in presymptomatic LoxSOD1^{G37R} mice, significant ($P < 0.05$; Student's t test) disease-associated inductions were identified in early symptomatic LoxSOD1^{G37R} mice for IGF-1 (2.0-fold), PTN (2.7-fold), and GDNF (8.6-fold), as well as a decrease in CNTF (2.3-fold), alterations that are comparable to those known to occur also after sciatic nerve injury (17, 19, 33, 34) (Fig. 5*B*). Importantly, whereas removal of mutant SOD1^{G37R} from Schwann cells did not influence disease-associated PTN, GDNF, or CNTF regulation, there was a complete lack of IGF-1 induction in sciatic nerves of LoxSOD1^{G37R}/P_0-cre mice as compared to LoxSOD1^{G37R} mice (Fig. 5*B*).

Discussion

In contrast to prior efforts with selective removal of a mutant *SOD1* gene from astrocytes (11) or microglia (10), each of which sharply slowed disease progression, our current findings have shown that similar removal of the same dismutase active mutant SOD1^{G37R} from Schwann cells accelerated the late phase of disease progression resulting in a disease course as aggressive as

that seen in a dismutase inactive mutant SOD1^{G85R} ALS mouse line. Our gene excision targeted 70% of axonal Schwann cells as well as 40% of terminal Schwann cells. When taken together with a prior demonstration that reduction of mutant SOD1 synthesis in muscle had no effect on any aspect of disease (16), our findings offer no support for an important role for mutant-derived toxicity within the non-neuronal cells at the neuromuscular junction. A further insight is that, in contrast to astrocytes and microglia, both muscle (16) and Schwann cells seem to be protected against the buildup of mutant SOD1 toxicity.

The most straightforward explanation for the unexpected protective role of Schwann cell-expressed mutant SOD1 in slowing disease progression is that the mutant we have tested (SOD1^{G37R}) retains fully functional dismutase activity (35). Indeed, ubiquitous overexpression of wild-type SOD1 in transgenic mice is neuroprotective against both cerebral ischemia (30) and spinal cord injury (31), whereas systemic SOD1 deletion in mice increased axotomy-induced motor neuron death (36). Dismutase inactive SOD1 mutant ALS mice would lack any Schwann cell-derived neuroprotective effect and should, therefore, have a more aggressive late disease phase. Indeed, retrospective analysis of survival data from our different ALS mouse cohorts revealed that dismutase inactive mutant SOD1^{G85R} (line 148) mice had a 2.5-fold shorter late phase (23.8 ± 4.6 d; $n = 20$) (29) compared with dismutase active mutant SOD1^{G37R} (line 106) mice (54.7 ± 6.4 d; $n = 20$) (28), despite similar survival times (12.5–13.5 months) (Fig. 2*D*). This more rapid disease progression in the dismutase inactive mutant was statistically highly significant ($P < 0.001$; Student's t test). A search of the literature revealed further support for such a correlation between dismutase activity and slow disease progression: disease in mice from dismutase inactive SOD1^{G127X} has a 2.5-fold shorter symptomatic disease phase than does a dismutase active SOD1^{G93A} line with similar survival times (37).

Although toxicity from a dismutase inactive mutant (SOD1^{G85R}) proceeds independent of overall dismutase activity provided by endogenous SOD1 (38), we suggest that during mutant SOD1-induced axonal degeneration, a cascade is triggered that produces reactive oxygen species at least some of which can be detoxified via SOD1 synthesized by Schwann cells. Potential sources of such reactive species include extracellular superoxide produced by mutant SOD1-dependent stimulation of NADPH oxidase in microglia/macrophages (6) and astrocytes (7) or from mutant SOD1 damage to mitochondria (4, 39, 40), especially in neurons. Indeed, mutant SOD1 damage within microglial/macrophages (10) or astrocytes (11) is known to drive rapid disease progression, findings that correlate well with our evidence here that Schwann cells depleted of a dismutase active mutant substantially shorten disease course. However, as Schwann cells are localized outside the spinal cord, the most likely sources for reactive oxygen species are (1) peripheral macrophages (which are known to invade degenerating peripheral nerves) (20), (2) Schwann cells themselves, or (3) the degenerating axons along which the Schwann cells are aligned.

Our hypothesis might be expected to predict a protective effect of (ubiquitously) overexpressing wild-type SOD1 in ALS mice, whereas no change (38) or a disease acceleration (41) have actually been reported. However, as toxicity of mutant SOD1 aggregates can be increased by wild-type SOD1 overexpression (41), protective effects within (nonsensitive) Schwann cells could have been masked in these prior efforts by increased toxicity within (sensitive) motor neurons, astrocytes, and/or microglia. Likewise, deletion of mouse SOD1 did not speed up disease in ALS mice (38), most probably due to similar opposing effects that neutralized each other or that the endogenous level of dismutase activity in Schwann cells was insufficient to provide a protective benefit.

Interestingly, increased disease duration in human ALS is correlated with increased stability of ALS-linked SOD1 mutants (42). As protein stability in general correlates with dismutase activity (35, 42), it is tempting to speculate that dismutase activity of Schwann cell-expressed SOD1 mutants is an important determinant of slowed disease progression in ALS. As a direct consequence, therapeutic down-regulation of dismutase active mutant SOD1 forms in familial ALS (43) should avoid Schwann cells.

A direct test of our hypothesis could be undertaken by selectively increasing wild-type SOD1 levels within Schwann cells, especially in ALS mice with a dismutase inactive mutant, such as SOD1^{G85R}. Such activity should prolong disease progression. Further, removal of mutant SOD1^{G85R} from Schwann cells would be predicted not to affect disease course. Interestingly, genetic deletion of *CCS1* (the enzyme responsible for loading SOD1 with the catalytic copper essential for dismutase activity) in mutant SOD1^{G37R} (line 29) ALS mice, led to slightly reduced survival (44) (and P.C. Wong; personal communications), consistent with a protective action of dismutase activity, although this effect was not visible in mutant SOD1^{G37R} (line 42) mice with very high levels of transgene expression (44).

Although linking the protective effect of Schwann cell-derived mutant SOD1^{G37R} to dismutase driven reduction of toxic superoxide is the most obvious explanation for our findings, reactive oxygen species, especially hydrogen peroxide (the product of the dismutase reaction), could also directly influence intracellular or intercellular signaling processes, including modulating transcription (45). Indeed, we found a disease-associated induction of IGF-1 transcripts in sciatic nerve Schwann cells of ALS mice, but this was completely abolished upon removal of mutant SOD1^{G37R} from those Schwann cells. Lack of IGF-1 induction was surprisingly selective after mutant SOD1 removal from Schwann cells, with responses of pleiotrophin, GDNF, and CNTF unaffected.

Moreover, although we detected much stronger disease-associated induction of GDNF than IGF-1, recent viral-mediated delivery of GDNF in ALS mice was much less efficient than IGF-1 (46). Thus, even a small loss of IGF-1 might have strong effects in ALS. Previous studies have already established the motor neuron protective potential of IGF-1 in ALS mice (46, 47) and IGF-1 synthesis by Schwann cells is known to be induced during axonal regeneration (34). As the degenerating sciatic nerve also contains invading macrophages (20), we cannot exclude them as a source of IGF-1 induction. In this case, mutant SOD1^{G37R} action (including damage) within Schwann cells could trigger secretion of paracrine acting factors (e.g., cytokines), which could initiate growth factor production in invading macrophages.

Nevertheless, what our evidence establishes is that this IGF-1 induction is dependent on mutant SOD1^{G37R} expression in Schwann cells, a finding that identifies Schwann cells—long overlooked in ALS—as participants in pathogenesis in familial SOD1-linked ALS and therefore establishing them as potential targets for therapeutic intervention in ALS.

Materials and Methods

Animals. All transgenic mouse lines were on a pure C57Bl/6 background. *Po-cre mice*: Mice heterozygous for a mP$_0$TOTA-Cre transgene that contains a complete mouse P$_0$-gene (*mpz*) with 6 kb of promotor, in which the ATG start of translation has been mutated and substituted with the Cre-recombinase gene (48). For additional details, see *SI Materials and Methods*.

Survival Analysis. Mice were weighed weekly as an objective and unbiased measure of disease course (10, 11, 28, 29). Additional details, see *SI Materials and Methods*.

For qPCR for mutant *SOD1* transgene levels, immunohistochemistry, morphometric analysis of axons, sciatic nerve regeneration measurements and RT-qPCR for sciatic nerve mutant *SOD1* and growth factor mRNA levels, see *SI Materials and Methods*.

Note. A study published after the manuscript from Keller et al. (40) provided additional evidence for the involvement of Schwann cells in ALS pathogenesis.

ACKNOWLEDGMENTS. We thank Drs. C. Svendsen and C. Vande Velde for essential discussions about growth factor dysregulations in Schwann cells; Drs. M. Garcia, U. Suter, S. Hunot, P.P. Michel, O. Corti, and E. Hirsch for helpful discussions; Drs. L. Wrabetz (San Raffaele Scientific Institute, Milan) and J. Chun (Scripps Research Institute, La Jolla, CA) for providing P_0-cre mice; Dr. R. Balice-Gordon for advice with terminal Schwann cell staining; Ms. J. Folmer for assistance with motor root tissue preparations; Ms. S. J. Chun, G. Szwajkowski, and K. Pytel for help with genotyping; Dr. S. Da Cruz for help with qPCR settings; and Dr. P. Soriano (Fred Hutchinson Cancer Research Center, Seattle) for ROSA26 reporter mice. This work was supported by National Institutes of Health (NIH) Grant NS 27036 (to D.W.C.) and a grant from the Packard Center for ALS Research (to D.W.C.). Additional support came from a Swiss National Science Foundation fellowship and a Neuropôle de Recherche Francilien fellowship (to C.S.L.); a Fondation pour la Recherche Medical fellowship, a Developmental grant from the Muscular Dystrophy Association, and an INSERM grant (to S.B.); a Japanese Ministry of Education, Culture, Sports, Science and Technology grant, a Japanese Health and Labour Sciences Research grant, and a Core Research for Evolutional Science and Technology of JST grant (to K.Y.). Salary support for D.W.C. was provided by the Ludwig Institute for Cancer Research. M.L.F. wishes to dedicate this work to the memory of Anna Maria Crespi Feltri.

1. Boillee S, Vande Velde C, Cleveland DW (2006) ALS: A disease of motor neurons and their nonneuronal neighbors. *Neuron* 52:39–59.
2. McNamara JO, Fridovich I (1993) Human genetics. Did radicals strike Lou Gehrig? *Nature* 362:20–21.
3. Rothstein JD, Martin LJ, Kuncl RW (1992) Decreased glutamate transport by the brain and spinal cord in amyotrophic lateral sclerosis. *N Engl J Med* 326:1464–1468.
4. Liu J, et al. (2004) Toxicity of familial ALS-linked SOD1 mutants from selective recruitment to spinal mitochondria. *Neuron* 43:5–17.
5. Urushitani M, et al. (2006) Chromogranin-mediated secretion of mutant superoxide dismutase proteins linked to amyotrophic lateral sclerosis. *Nat Neurosci* 9:108–118.
6. Harraz MM, et al. (2008) SOD1 mutations disrupt redox-sensitive Rac regulation of NADPH oxidase in a familial ALS model. *J Clin Invest* 118:659–670.
7. Marchetto MC, et al. (2008) Non-cell-autonomous effect of human $SOD1^{G37R}$ astrocytes on motor neurons derived from human embryonic stem cells. *Cell Stem Cell* 3:649–657.
8. Nishitoh H, et al. ALS-linked mutant SOD1 induces ER stress- and ASK1-dependent motor neuron death by targeting Derlin-1. *Genes Dev* 22:1451–1464, 2008.
9. Clement AM, et al. (2003) Wild-type nonneuronal cells extend survival of SOD1 mutant motor neurons in ALS mice. *Science* 302:113–117.
10. Boillee S, et al. (2006) Onset and progression in inherited ALS determined by motor neurons and microglia. *Science* 312:1389–1392.
11. Yamanaka K, et al. (2008) Astrocytes as determinants of disease progression in inherited amyotrophic lateral sclerosis. *Nat Neurosci* 11:251–253.
12. Di Giorgio FP, Boulting GL, Bobrowicz S, Eggan KC (2008) Human embryonic stem cell-derived motor neurons are sensitive to the toxic effect of glial cells carrying an ALS-causing mutation. *Cell Stem Cell* 3:637–648.
13. Di Giorgio FP, Carrasco MA, Siao MC, Maniatis T, Eggan K (2007) Non-cell autonomous effect of glia on motor neurons in an embryonic stem cell-based ALS model. *Nat Neurosci* 10:608–614.
14. Nagai M, et al. (2007) Astrocytes expressing ALS-linked mutated SOD1 release factors selectively toxic to motor neurons. *Nat Neurosci* 10:615–622.
15. Dobrowolny G, et al. (2008) Skeletal muscle is a primary target of $SOD1^{G93A}$-mediated toxicity. *Cell Metab* 8:425–436.
16. Miller TM, et al. (2006) Gene transfer demonstrates that muscle is not a primary target for non-cell-autonomous toxicity in familial amyotrophic lateral sclerosis. *Proc Natl Acad Sci USA* 103:19546–19551.
17. Hoke A (2006) Neuroprotection in the peripheral nervous system: rationale for more effective therapies. *Arch Neurol* 63:1681–1685.
18. Woodhoo A, Sommer L (2008) Development of the Schwann cell lineage: from the neural crest to the myelinated nerve. *Glia* 56:1481–1490.
19. Chen ZL, Yu WM, Strickland S (2007) Peripheral regeneration. *Annu Rev Neurosci* 30:209–233.
20. Martini R, Fischer S, Lopez-Vales R, David S (2008) Interactions between Schwann cells and macrophages in injury and inherited demyelinating disease. *Glia* 56:1566–1577.
21. Scherer SS, Wrabetz L (2008) Molecular mechanisms of inherited demyelinating neuropathies. *Glia* 56:1578–1589.
22. Perrie WT, et al. (1993) Changes in the myelinated axons of femoral nerve in amyotrophic lateral sclerosis. *J Neural Transm Suppl* 39:223–233.
23. De Winter F, et al. (2006) The expression of the chemorepellent Semaphorin 3A is selectively induced in terminal Schwann cells of a subset of neuromuscular synapses that display limited anatomical plasticity and enhanced vulnerability in motor neuron disease. *Mol Cell Neurosci* 32:102–117.
24. Pun S, Santos AF, Saxena S, Xu L, Caroni P (2006) Selective vulnerability and pruning of phasic motoneuron axons in motoneuron disease alleviated by CNTF. *Nat Neurosci* 9:408–419.
25. Schaefer AM, Sanes JR, Lichtman JW (2005) A compensatory subpopulation of motor neurons in a mouse model of amyotrophic lateral sclerosis. *J Comp Neurol* 490:209–219.
26. Feltri ML, et al. (2002) Conditional disruption of beta 1 integrin in Schwann cells impedes interactions with axons. *J Cell Biol* 156:199–209.
27. Bolis A, et al. (2005) Loss of Mtmr2 phosphatase in Schwann cells but not in motor neurons causes Charcot-Marie-Tooth type 4B1 neuropathy with myelin outfoldings. *J Neurosci* 25:8567–8577.
28. Lobsiger CS, Garcia ML, Ward CM, Cleveland DW (2005) Altered axonal architecture by removal of the heavily phosphorylated neurofilament tail domains strongly slows superoxide dismutase 1 mutant-mediated ALS. *Proc Natl Acad Sci USA* 102:10351–10356.
29. Lobsiger CS, Boillee S, Cleveland DW (2007) Toxicity from different SOD1 mutants dysregulates the complement system and the neuronal regenerative response in ALS motor neurons. *Proc Natl Acad Sci USA* 104:7319–7326.
30. Saito A, Hayashi T, Okuno S, Ferrand-Drake M, Chan PH (2003) Overexpression of copper/zinc superoxide dismutase in transgenic mice protects against neuronal cell death after transient focal ischemia by blocking activation of the bad cell death signaling pathway. *J Neurosci* 23:1710–1718.
31. Sugawara T, Lewen A, Gasche Y, Yu F, Chan PH (2002) Overexpression of SOD1 protects vulnerable motor neurons after spinal cord injury by attenuating mitochondrial cytochrome c release. *FASEB J* 16:1997–1999.
32. Islamov RR, et al. (2002) 17Beta-estradiol stimulates regeneration of sciatic nerve in female mice. *Brain Res* 943:283–286.
33. Sendtner M, Stockli KA, Thoenen H (1992) Synthesis and localization of ciliary neurotrophic factor in the sciatic nerve of the adult rat after lesion and during regeneration. *J Cell Biol* 118:139–148.
34. Sullivan KA, Kim B, Feldman EL (2008) Insulin-like growth factors in the peripheral nervous system. *Endocrinology* 21:21–31.
35. Borchelt DR, et al. (1994) Superoxide dismutase 1 with mutations linked to familial amyotrophic lateral sclerosis possesses significant activity. *Proc Natl Acad Sci USA* 91:8292–8296.
36. Reaume AG, et al. (1996) Motor neurons in Cu/Zn superoxide dismutase-deficient mice develop normally but exhibit enhanced cell death after axonal injury. *Nat Genet* 13:43–47.
37. Jonsson PA, et al. (2004) Minute quantities of misfolded mutant superoxide dismutase-1 cause amyotrophic lateral sclerosis. *Brain* 127:73–88.
38. Bruijn LI, et al. (1998) Aggregation and motor neuron toxicity of an ALS-linked SOD1 mutant independent from wild-type SOD1 *Science* 281:1851–1854.
39. Vande Velde C, Miller TM, Cashman NR, Cleveland DW (2008) Selective association of misfolded ALS-linked mutant SOD1 with the cytoplasmic face of mitochondria. *Proc Natl Acad Sci USA* 105:4022–4027. Epub 2008 Feb 4022.
40. Vijayvergiya C, Beal MF, Buck J, Manfredi G (2005) Mutant superoxide dismutase 1 forms aggregates in the brain mitochondrial matrix of amyotrophic lateral sclerosis mice. *J Neurosci* 25:2463–2470.
41. Deng HX, et al. (2006) Conversion to the amyotrophic lateral sclerosis phenotype is associated with intermolecular linked insoluble aggregates of SOD1 in mitochondria. *Proc Natl Acad Sci USA* 103:7142–7147.
42. Sato T, et al. (2005) Rapid disease progression correlates with instability of mutant SOD1 in familial ALS. *Neurology* 65:1954–1957.
43. Smith RA, et al. (2006) Antisense oligonucleotide therapy for neurodegenerative disease. *J Clin Invest* 116:2290–2296.
44. Subramaniam JR, et al. (2002) Mutant SOD1 causes motor neuron disease independent of copper chaperone-mediated copper loading. *Nat Neurosci* 5:301–307.
45. Veal EA, Day AM, Morgan BA (2007) Hydrogen peroxide sensing and signaling. *Mol Cell* 26:1–14.
46. Kaspar BK, Llado J, Sherkat N, Rothstein JD, Gage FH (2003) Retrograde viral delivery of IGF-1 prolongs survival in a mouse ALS model. *Science* 301:839–842.
47. Dobrowolny G, et al. (2005) Muscle expression of a local Igf-1 isoform protects motor neurons in an ALS mouse model. *J Cell Biol* 168:193–199.
48. Feltri ML, et al. (1999) P0-Cre transgenic mice for inactivation of adhesion molecules in Schwann cells. *Ann NY Acad Sci* 883:116–123.
49. Keller AF, Gravel M, Kriz J (2008) Live imaging of amyotrophic lateral sclerosis pathogenesis: Disease onset is characterized by marked induction of GFAP in Schwann cells. *Glia*, in press.

Supporting Information

Lobsiger et al. 10.1073/pnas.0813339106

SI Materials and Methods

Animals. All transgenic mouse lines were on a pure C57BL/6 background.

P_0-cre mice. Mice heterozygous for a mP_0TOTA-Cre transgene, which contains a complete mouse P_0-gene (*mpz*) with 6 kb of promoter, in which the ATG start of translation has been mutated and substituted with the Cre-recombinase gene (1).

ROSA26 reporter mice. Heterozygous mice that ubiquitously express a β-galactosidase (β-Gal) transgene that can be translated into functional β-Gal only if a Cre-mediated recombination removes a premature translation terminator (ROSA26-lox-STOP-lox-β-Gal; generated via homologous recombination and "knock-in" into the ROSA26 locus) (2).

LoxSOD1^{G37R} ALS mice. Mice heterozygous for a 12 kb genomic DNA fragment encoding the human *SOD1^{G37R}* transgene, under its endogenous promoter, flanked by loxP sequences (3).

Additional ALS mouse lines. Heterozygous mutant SOD1^{G85R} (Line 148) (4) and heterozygous mutant SOD1^{G37R} (line 106) (5) mice.

Survival analysis. Heterozygous P_0-cre mice were mated to heterozygous LoxSOD1^{G37R} ALS mice and resulting LoxSOD1^{G37R}/P_0-cre mice were compared with LoxSOD1^{G37R} littermates. Numbers of progeny were as expected by Mendelian transmissions and genotyping was performed as previously described (1, 3). Mice were weighted weekly as an objective and unbiased measure of disease course (3, 6–9). Time of disease onset was retrospectively determined as the time when mice reached peak body weight. We previously proposed that decline in peak body weight as the earliest observable measure of disease onset because there is high degree of correlation between the age at which Rotarod performance declines and the initial loss of body weight (10). Indeed, as subsequently confirmed by others, peak body weight before weight loss is an objective, easily measured parameter that defines the earliest disease onset, initiating before any observable motor performance decline, such as grip strength, Rotarod performance, and cage activity (11, 12). The time of early disease was defined at the time when denervation-induced muscle atrophy had produced a 10% loss of maximal weight (which is accompanied by gait alterations and failure of hind limb splaying reflex, without obvious signs of paralysis). This early disease is followed by the appearance of progressive paralysis. During the symptomatic phase, mice were observed daily and end stage was defined by paralysis so severe that the animal could not right itself within 20 seconds when placed on its side, an endpoint frequently used for SOD1 mutant expressing mice (3, 6–9) and one that was consistent with the requirements of the Animal Care and Use Committee of the University of California. At this stage, ALS mice will die within 24 hours and were therefore killed. The early or late phase of disease progression was defined by the duration between the onset and early disease or between early disease and end stage, respectively.

Real-Time PCR Analysis of Mutant SOD1 Transgene Levels. Freshly isolated sciatic nerves or spinal cords were digested overnight at 55° C in 500 μl of 10 mM Tris (pH 7.4), 100 mM NaCl, 10 mM EDTA (pH 8), and 0.5% SDS with 10 μl of Proteinase K (20 mg/ml). Genomic DNA was extracted by phenol/chloroform and ethanol precipitation. One sciatic nerve yielded 3–3.5 μg of genomic DNA. Mouse apolipoprotein B (*apob*) was used as a normalizer gene. Genomic DNA (40 ng) was amplified with iQ Supermix (Bio-Rad) and 100 nM of each primer and probe in a Bio-Rad iCycler real-time PCR machine: 1 cycle 50° C, 2 min; 1 cycle 95° C, 10 min; 40 cycles 95° C, 15 sec, 60° C 1 min. Human *SOD1* transgene levels were normalized to mouse apolipoprotein B (*apob*) gene levels (3). *SOD1* and *apob* primer/probe sets were run in the same reaction, with every reaction run in triplicates and all samples run in parallel. The entire experiment was repeated twice and results were averaged. Specific primers and probes were (3): human *SOD1*-forward, CAATGTGACTGCTGACAAAG; human *SOD1*-reverse, GTGCGGCCAATGATGCAAT; human *SOD1*-probe, fam-CCGATGTGTCTATTGAAGATTCTG-BHQ; *apob*-forward, CACGTGGGCTCCAGCATT; *apoB*-reverse, TCACCAGTCATTTCTGCCTTTG; *apob*-probe, Texas Red-CCAATGGTCGGGCACTGCTCAA-BHQ2.

Real-Time RT-PCR Analysis of Sciatic Nerve Mutant SOD1 and Growth Factor mRNA Levels. Total RNA was isolated from freshly dissected sciatic nerves (2 per mouse; 1.5-cm long piece starting at the gastrocnemius muscle) by using the RNeasy Mini Lipid Kit (Qiagen) with DNase treatment. Tissues were lysed in 1 ml QIAzol Lysis Reagent (Qiagen) by using a Polytron (IKA-Werke GMBH, Germany). Two sciatic nerves yielded 1.5–2 μg of total RNA. RNA quality was determined with a BioAnalyzer 2100 (Agilent) and RIN-values were between 7 and 8. cDNA was generated from 450 ng of total RNA by using SuperScript-III (Invitrogen) and 1/40 was amplified with iQ SYBR Green Supermix (Bio-Rad) and 100 nM of each primer in a iCycler: 1 cycle 50° C, 2 min; 1 cycle 95° C, 10 min; 40 cycles 95° C, 15 sec, 60° C 1 min. Mouse gamma actin (*actg1*) was used as a normalizer gene. Human *SOD1*, mouse *igf1*, mouse *gdnf*, mouse *cntf,* and mouse *ptn* cDNA levels were normalized to *actg1* cDNA levels. Every gene was run in parallel with the *actg1* normalizer, with every reaction run in triplicates. All samples for a specific gene were run in parallel. The experiment for every gene was run twice and results were averaged. Specific primers were: *SOD1*-forward, AGGGCATCATCAATTTCGAG; *SOD1*-reverse, ACATTGCCCAAGTCTCCAAC; *igf1* (SA-PPM03387A) and *gdnf* (SA-PPM04315A) were both from SuperArray (SABiosciences, Frederick, MD); *cntf*-forward, TGGCTAGCAAGGAAGATTCG; *cntf*-reverse, CATCTCACTCCAGCGATCAG; *ptn*-forward, TTTTCATCTTGGCAGCTGTG; *ptn*-reverse, ACACTCCACTGCCATTCTCC; *actg1*-forward, TGGATCAGCAAGCAGGAGTATG; *actg1*-reverse, CCTGCTCAGTCCATCTAGAAGCA.

Immunohistochemistry. For tissue collection, mice were perfused with 4% paraformaldehyde. Spinal cords and gastrocnemius muscles were cryoprotected and snap frozen in isopropanol in TissueTek (Sakura). Thirty μm spinal cord and 40 μm muscle cryosections were used and β-galactosidase activity was measured by overnight incubation with X-Gal (5-bromo-4-chloro-3-indolyl-D-galactoside) substrate (0.2 mg/ml) in PBS containing 4 mM potassium ferrocyanide, 4 mM potassium ferricyanide and 1 mM magnesium chloride followed by counterstaining in eosin for 1 min. To identify terminal Schwann cells, after X-Gal staining, muscle sections were incubated in PBS/0.3% Triton-X100 overnight with a polyclonal rabbit antibody against S100β (1/200; Dako, Carpinteria, CA) followed by biotinylated species-specific secondary antibodies. The staining was revealed by the avidin-biotin complex immunoperoxidase technique (Vectastain ABC kit, Vector Laboratories, Burlingame, CA, 1:500 in PBS) and the diaminobenzidine chromogen (Vector Laboratories). Sections were dehydrated and mounted with Permount medium (Fisher Scientific).

Morphometric Analysis of Axons. Mice were perfused with 4% paraformaldehyde and L5 roots or entire sciatic nerves were dissected.

For motor root morphology. L5 roots transversely sectioned into 5 mm blocks, were treated with 2% osmium tetroxide in 0.05 M cacodylate buffer, washed, dehydrated, and embedded with Epon (Electron Microscopy Sciences). One-micrometer-thick cross sections were cut and stained with 1% toluidine blue, 1% sodium borate for 30 seconds, rinsed and dried (6). Both L5 motor roots from each animal were counted, averaged and axonal caliber distributions were determined as described (6).

For longitudinal nerve sections. Five-millimeter-long sciatic nerve pieces (chosen distally; the last 5 mm before entering the gastrocnemius muscle) were embedded and treated as for the L5 roots.

Sciatic Nerve Regeneration Measurements. Mice were placed under metophane anesthesia and the sciatic nerve was exposed via an incision in the flank followed by separation of underlying musculature by blunt dissection. The nerve was crushed (twice for 20 seconds at the same location) by using fine jewelers forceps at the level of the obturator tendon. To assess functional recovery of the injured limb, the mouse was induced to spread its toes by briefly lifting the hind limbs off the bench. Distance from first to fifth digits was measured daily with a divider for both the injured and uninjured leg.

1. Feltri ML, et al. (1999) P0-Cre transgenic mice for inactivation of adhesion molecules in Schwann cells. *Ann NY Acad Sci* 883:116–123.
2. Soriano P (1999) Generalized lacZ expression with the ROSA26 Cre reporter strain. *Nat Genet* 21:70–71.
3. Boillee S, et al. (2006) Onset and progression in inherited ALS determined by motor neurons and microglia. *Science* 312:1389–1392.
4. Bruijn LI, et al. (1997) ALS-linked SOD1 mutant G85R mediates damage to astrocytes and promotes rapidly progressive disease with SOD1-containing inclusions. *Neuron* 18:327–338.
5. Wong PC, et al. (1995) An adverse property of a familial ALS-linked SOD1 mutation causes motor neuron disease characterized by vacuolar degeneration of mitochondria. *Neuron* 14:1105–1116.
6. Lobsiger CS, Garcia ML, Ward CM, Cleveland DW (2005) Altered axonal architecture by removal of the heavily phosphorylated neurofilament tail domains strongly slows superoxide dismutase 1 mutant-mediated ALS. *Proc Natl Acad Sci USA* 102:10351–10356.
7. Lobsiger CS, Boillee S, Cleveland DW (2007) Toxicity from different SOD1 mutants dysregulates the complement system and the neuronal regenerative response in ALS motor neurons. *Proc Natl Acad Sci USA* 104:7319–7326.
8. Yamanaka K, et al. (2008) Astrocytes as determinants of disease progression in inherited amyotrophic lateral sclerosis. *Nat Neurosci* 11:251–253.
9. Miller TM, et al. (2006) Gene transfer demonstrates that muscle is not a primary target for non-cell-autonomous toxicity in familial amyotrophic lateral sclerosis. *Proc Natl Acad Sci USA* 103:19546–19551.
10. Liu J, Shinobu LA, Ward CM, Young D, Cleveland DW (2005) Elevation of the Hsp70 chaperone does not effect toxicity in mouse models of familial amyotrophic lateral sclerosis. *J Neurochem* 93:875–882.
11. Schutz B, et al. (2005) The oral antidiabetic pioglitazone protects from neurodegeneration and amyotrophic lateral sclerosis-like symptoms in superoxide dismutase-G93A transgenic mice. *J Neurosci* 25:7805–7812.
12. Matsumoto A, et al. (2006) Disease progression of human SOD1 (G93A) transgenic ALS model rats. *J Neurosci Res* 83:119–133.
13. Islamov RR, et al. (2002) 17Beta-estradiol stimulates regeneration of sciatic nerve in female mice. *Brain Res* 943:283–286.

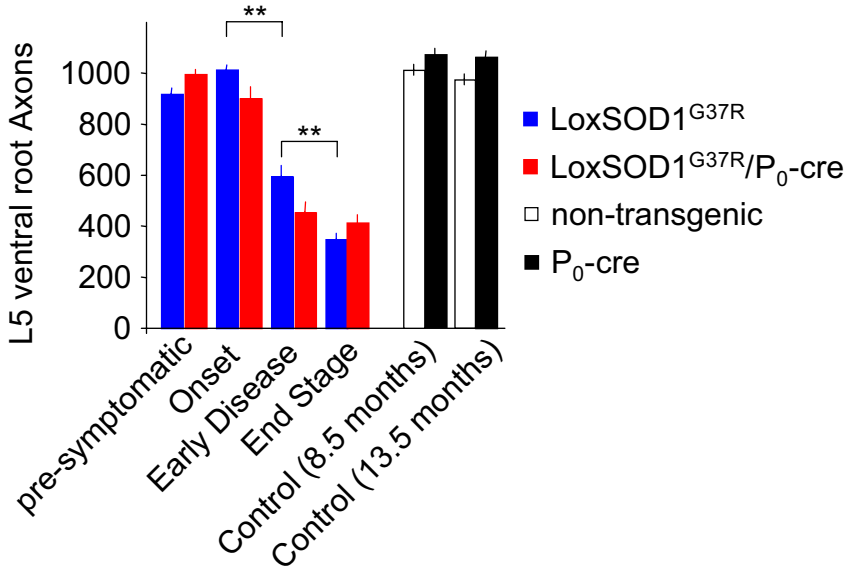

Fig. S1. Quantitative analysis of axonal degeneration in lumbar motor roots of ALS mice with or without Cre-mediated mutant SOD1 excision in Schwann cells. Numbers of axons in L5 motor roots of LoxSOD1^{G37R} and LoxSOD1^{G37R}/P_0-cre at presymptomatic (at 4 months) and onset (8.5 months) time points and at early disease and end stage. No axonal degeneration was seen in nontransgenic or single transgenic P_0-cre control mice at ages matched to onset (8.5 months) or end stage (13.5 months) ($n = 4$ mice per group; error, SEM; **, $P < 0.01$; Student's t test).

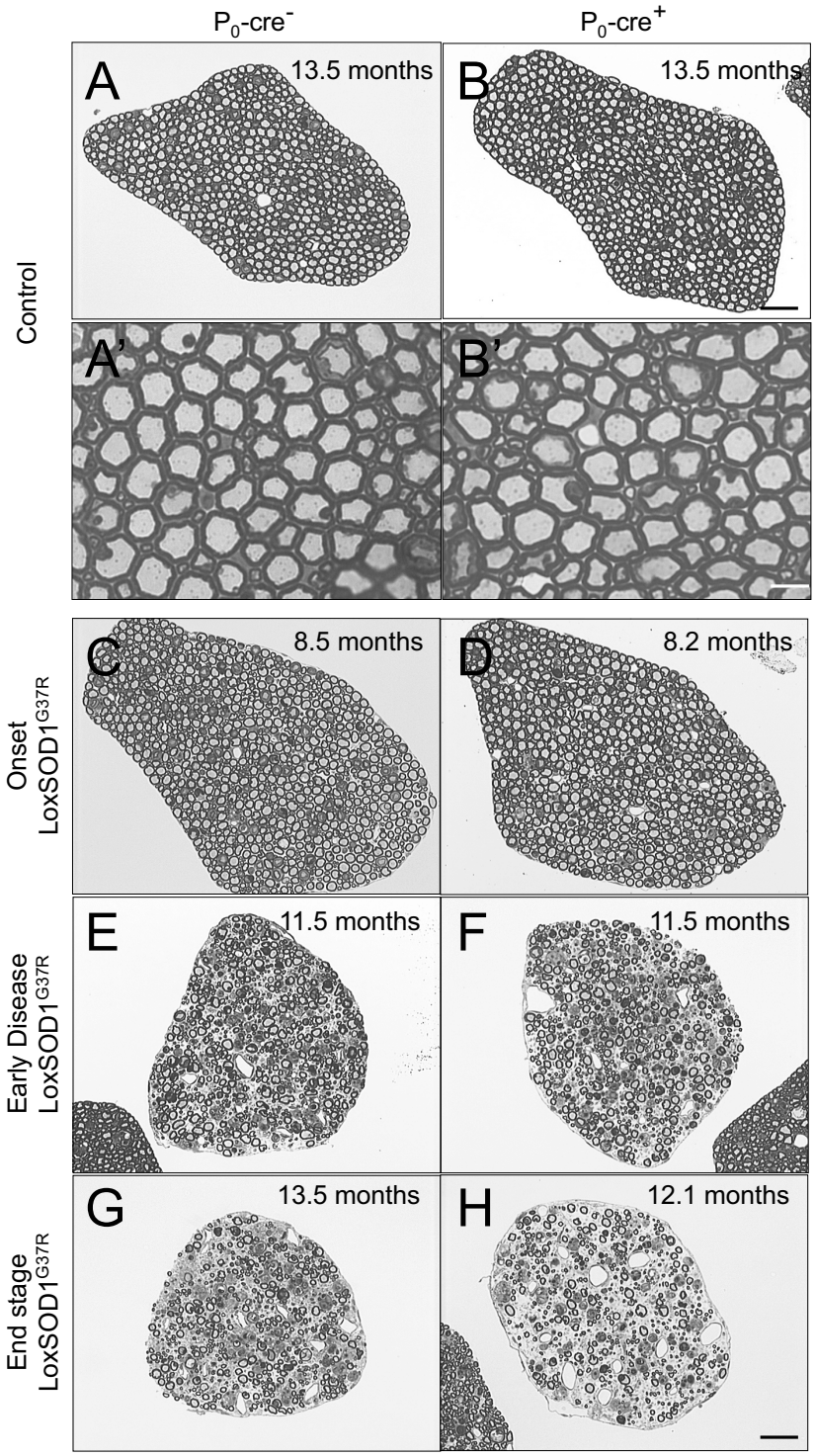

Fig. S2. Morphological assessment of axonal and myelin degeneration in lumbar motor roots of ALS mice with or without Cre-mediated mutant SOD1 excision in Schwann cells. (*A–H*) Toluidine-blue staining of semithin cross-sections from L5 motor root axons are shown. Nontransgenic (P_0-cre$^-$) (*A*) and single transgenic P_0-cre$^+$ (*B*) control mice show no signs of axonal degeneration (*A* and *B*) and qualitatively normal axon calibers and myelin thickness (enlargement [*A′* and *B′*]) at advanced ages matched to end stage of ALS mice (13.5 months). (*C–H*) Removal of dismutase *active* mutant SOD1^{G37R} from Schwann cells do not influence onset (weight peak) (*C* and *D*) or early disease (10% weight loss) (*E* and *F*) of LoxSOD1^{G37R} ALS-mice. However, end stage (paralysis) and resulting end stage pathology are reached significantly *earlier* in LoxSOD1^{G37R}/P_0-cre mice (*H*) as compared with LoxSOD1^{G37R} mice (*G*). Indicated are average ages at which LoxSOD1^{G37R}/P_0-cre (*D*, *F*, *H*) and LoxSOD1^{G37R} (*C*, *E*, *G*) mice reach the respective disease stages. [Scale bars: 100 μm (*A–H*) and 10 μm (*A′* and *B′*).]

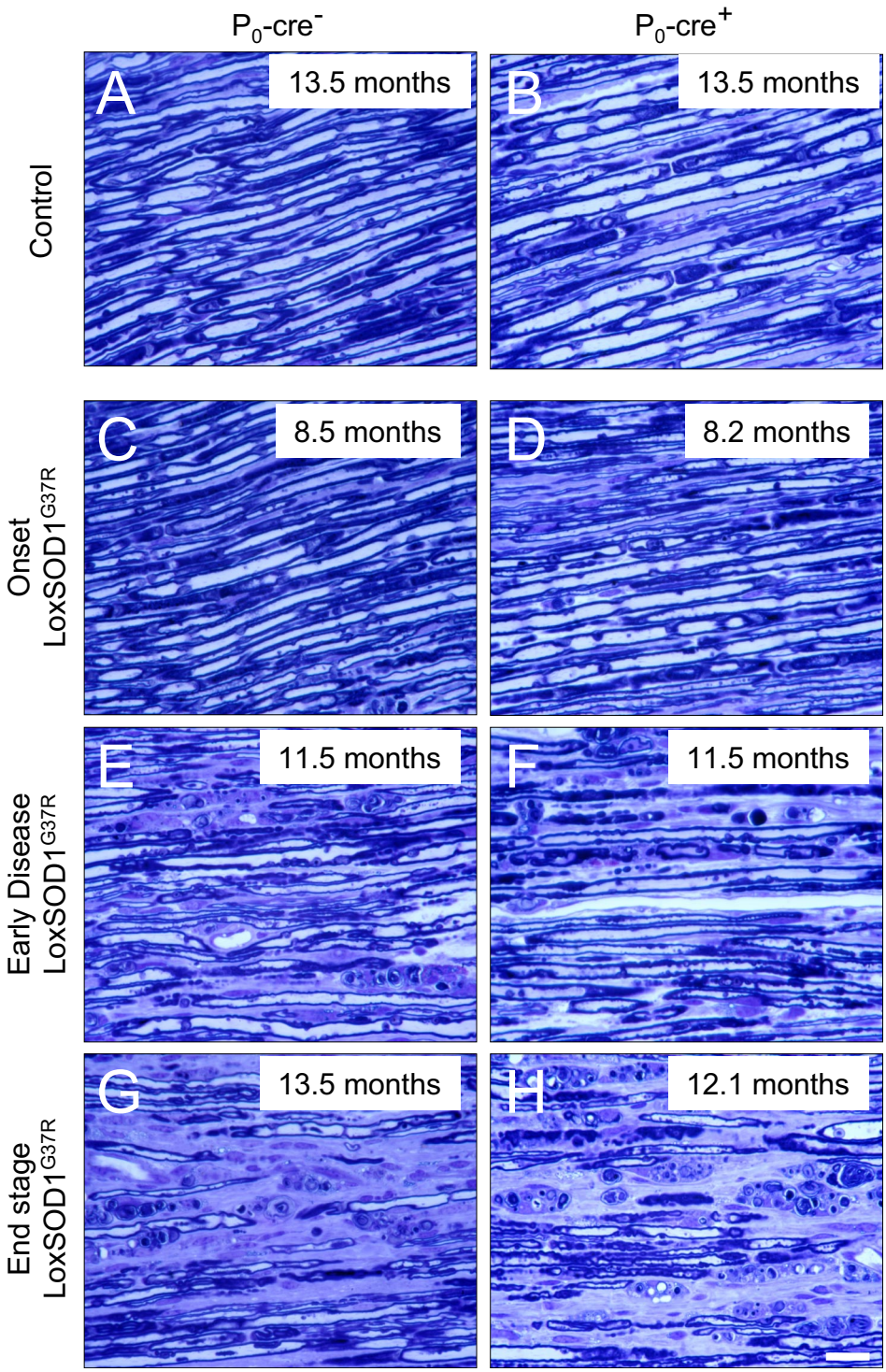

Fig. S3. Morphological assessment of axonal and myelin degeneration in sciatic nerves of ALS mice with or without Cre-mediated mutant SOD1 excision in Schwann cells. (*A–H*) Similar to Fig. S2 but instead, toluidine-blue staining of semithin longitudinal-sections of distal sciatic nerves are shown.

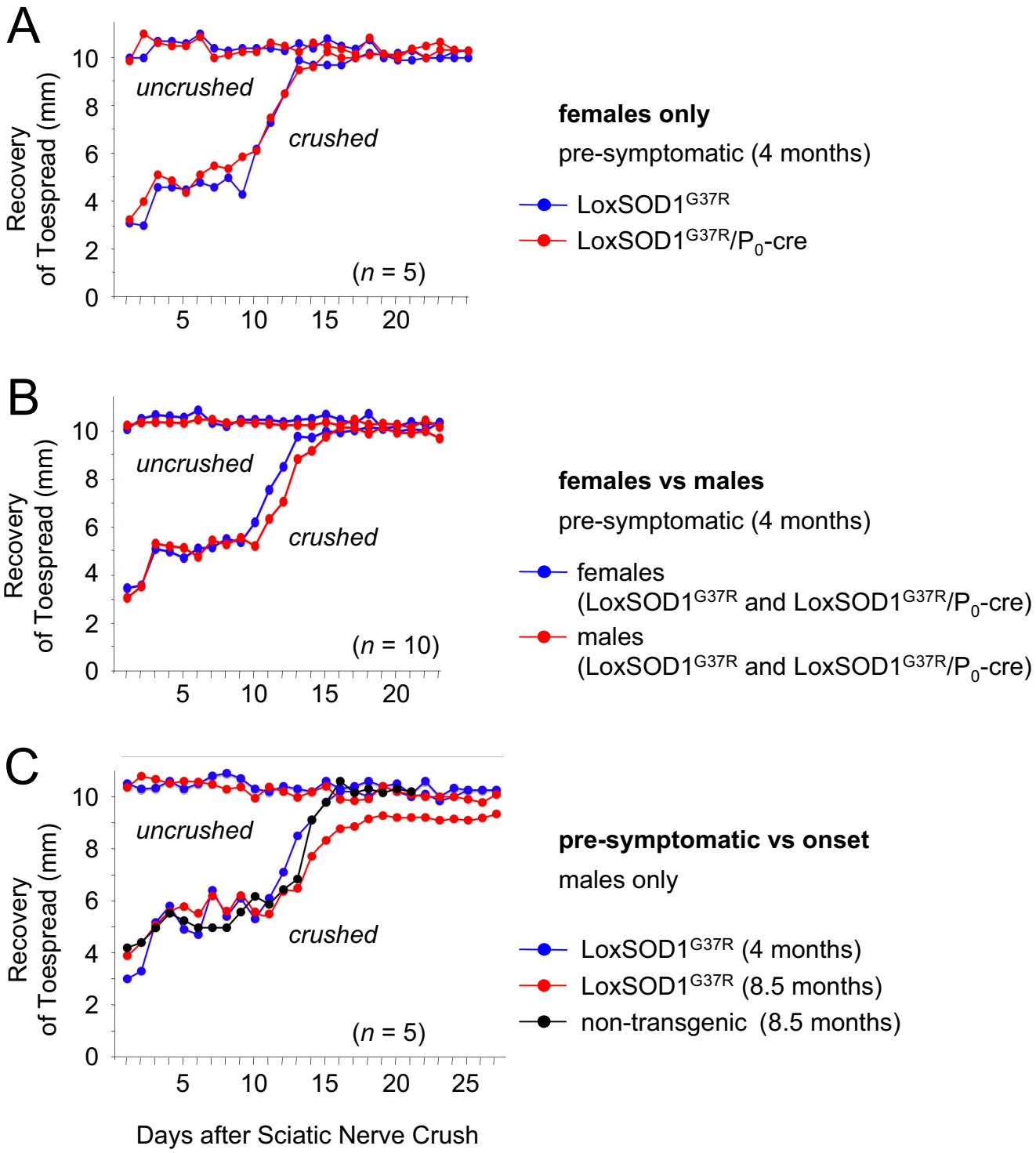

Fig. S4. Influence of presence of mutant SOD1 in Schwann cells, sex and disease stage on axonal regeneration after sciatic nerve crush in ALS mice. (*A*) Like for males (Fig. 4*A*) the speed of nerve regeneration (measured by the toe spread) after unilateral crush injury was not significantly different between presymptomatic (4-month-old) female LoxSOD1^{G37R}/P_0-cre and LoxSOD1^{G37R} ALS mice (n = 5 mice per group). (*B*) Nerve regeneration was slightly faster in presymptomatic (4-month-old) female than in male ALS mice (n = 10 mice per group; per group data from five LoxSOD1^{G37R} and five LoxSOD1^{G37R}/P_0-cre ALS mice were averaged), consistent with previous findings that estrogen is neuroprotective and that regeneration in (nontransgenic) females is faster than in males (13). (*C*) Disease associated slowing of nerve regeneration in LoxSOD1^{G37R} ALS mice at onset (8.5 months old) as compared with presymptomatic (4 months old) LoxSOD1^{G37R} ALS mice. This effect was not due to normal aging, as 8.5-month-old nontransgenic control mice did not show a slower regeneration (n = 5 mice per group; only males used).